

# Force Feedback Analysis: Friction Stir Welding of Aluminium Metal Matrix Composite

Olayinka O. Abegunde *Member, IAENG*, Esther T. Akinlabi, *Member, IAENG* and Daniel M. Madyira, *Member, IAENG*

**Abstract** — This paper presents the output response parameters (forces feedback, torque and heat input) during friction stir welding of aluminium. The welding was performed on an Intelligent Stir Welding for Industry and Research (I-STIR) Process Development System (PDS) using different rotational and transverse speeds while other input parameters like tool geometry, tilt angle and workpieces configuration were kept constant. The I-STIR FSW platform is capable of recording the force feedback and torque during the welding process and the heat input was calculated using a mathematical relationship. The study reveals the influence of the rotational and transverse speed on the pattern of the output feedback. The reinforcement ceramic particles added to the weld seam during welding also affected the output feedback.

**Index Terms**—Force feedback, Friction Stir Welding, Heat input, Torque.

## I. INTRODUCTION

Friction stir welding (FSW) is a solid state welding process initially developed for joining aluminium alloys but overtime, it has been used on other metals like magnesium, copper, steel and titanium [1]. The FSW process can be categorized into pre-welding and welding stages. During pre-welding, a rotating non-consumable tool is plunged downward into the workpiece in the z-direction (plunging state) at predefined process variables. In the welding stage, the tool rotates for a while in the same spot to soften the workpieces by frictional heating (dwelling time) and then, the tool starts to travel in a longitudinal x-direction (welding direction), stirring and joining the workpieces together [2].

Manuscript received February 11, 2016; revised March 06, 2016. This work was supported and financed by the University of Johannesburg under the Global Excellence Stature (GES) award Scholarship award of Postgraduate Research Centre.

O. O. Abegunde is a Masters Candidate in the Department of Mechanical Engineering Science, University of Johannesburg, Auckland Park Kingsway Campus, Johannesburg, South Africa, 2006. (Phone: +27620320634; E-mail: yinkaabeegs@ymail.com: oabegunde@uj.ac.za).

E. T. Akinlabi is an Associate Professor and the Head of Department in the Department of Mechanical Engineering Science, University of Johannesburg, Auckland Park Kingsway Campus, Johannesburg, South Africa, 2006. (E-mail: etakinlabi@uj.ac.za).

D. M. Madyira is a Lecturer in the Department of Mechanical Engineering Science, University of Johannesburg, Auckland Park Kingsway Campus, Johannesburg, South Africa, 2006. (E-mail: dmadyira@uj.ac.za).

For successful welds to be achieved, the relationship of the process variables is fundamental and must be understood.

These process variables can be classified as input and output parameters. The independent input parameters are the tool, workpiece and process parameters (rotational and transverse speed) while the outputs are force, torque, power and heat input. The output parameters are functions of the aforementioned input parameters and play significant roles in the final weld matrix.

The tool in FSW experiences forces in three coordinate axis namely longitudinal or transverse force  $F_x$ , lateral force  $F_y$  and downward force  $F_z$  due to rotational and linear movement of the tool. These output parameters act around the tool on the workpiece and vary with the process parameters, the tool and composition of the workpiece [3].

During FSW, torque is an indicator of shear stress around the tool which is required to rotate the tool, the amount of which relies on the friction coefficient, force response and the flow strength of the material in the surrounding region. Reducing torque minimizes the total power required, thus enhancing the energy efficiency. A downward force, ( $F_z$ ), is necessary to maintain the position of the tool at or below the material surface and lateral force, ( $F_y$ ) acts perpendicularly to the tool traverse direction. The longitudinal force, ( $F_x$  or X-force) acts parallel to the tool motion and is positive in the traverse direction. Since this force arises as a result of the resistance of the material to the motion of the tool, it is expected that this force will decrease as the temperature of the material around the tool is increased. X-force can also indicate tool failure. Excessive X-force will cause tool failure [4, 5] while the  $F_y$  acts perpendicular to the tool in transverse direction [6]. Torque decreases with increasing rotation speed due to higher temperature caused by higher heat generation rate (heat input/time), whose indicator is power input [7].

At the pre-welding stage, when the rotating tool is plunged into the work pieces, the downward force rises while the tool drills a hole in the work pieces forming a region of severely deformed material due to the tool/material interaction. Presented in Figure 1 is a typical force feedback of the downward force against time during FSW. The first spike shown is caused by fast plummet of the tool into the work pieces; this is referred to as the tool plunge phase. After the plunge, a certain time period elapses, referred to as the dwell time where the tool rotates in the work pieces, but with no traverse. This generates the initial heat to plasticize the material before the traverse is started. At the end of the dwell time, the tool traverses and a ramp up occurs due to forging resulting in an increase in the downward vertical

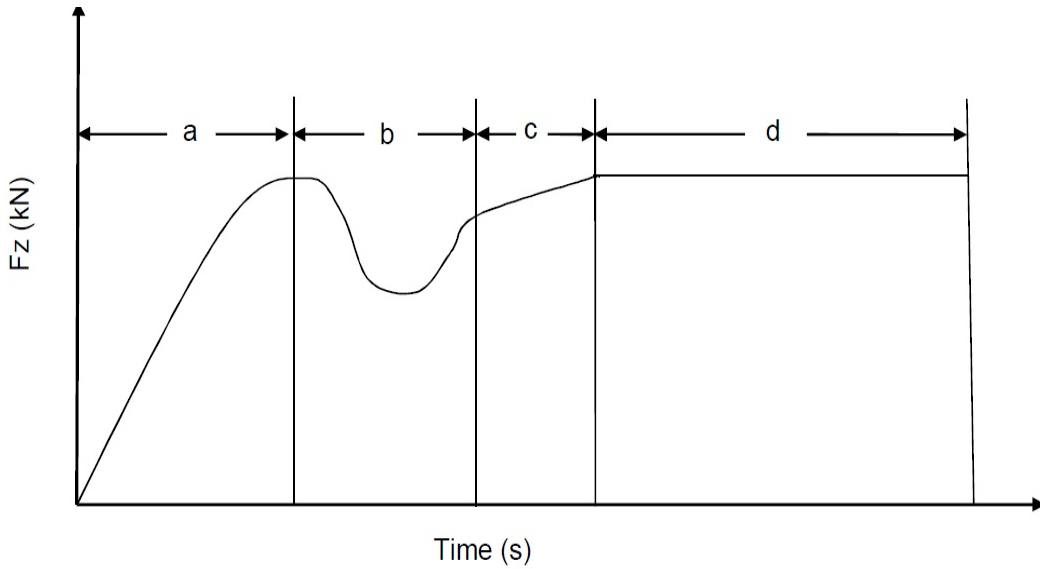


Fig. 1. Typical force feedback plot of vertical downward force ( $F_z$ ) with respect to time Where, a = tool plunge, b = dwell time, c = ramp up, d = steady state weld region [7].

force. Then, a stable vertical downward force is achieved in the welding where all the welding parameters are nearly constant. This period can be referred to as the steady state of the welding process, i.e., the period during which the force, torque and heat reach a near equilibrium state [7, 8].

Studies have been conducted to understand the relationship that existed between the process variables using both experimental, empirical and analytical models. Blignault et al [9] discussed the development of a multi-axial transducers capable of capturing the process forces footprint which can be employed to measure the energy input to FSW. Arbogast [10] experimentally demonstrated the change in process forces due to clamping locations, welding direction, crossing over pre-existing FSW and changing the process parameters (rotation rate and traverse speed). Hattingsh et al [11] have also studied the relationship among tool profile, rotational rate, traverse speed and microstructure using force footprint plots. They developed polar plots that show the force vector experienced by the tool during each revolution. Long and Reynolds [12] studied the effects of varying material properties and process parameters on the trends in x axis forces and potential weld defect formation (via a material flow pattern) by fluid dynamics simulation. Balasubramanian [13] also reported the process forces during friction stir welding of aluminium alloys and concluded that the forces during FSW can help in understanding the flow of materials and predict the occurrence of voids in the nugget.

This research study concentrates on giving more insight into the relationship of process variables and to develop an understanding of the relationship between the transverse speed, rotational speed, force input, torque and heat input during FSW.

## II. EXPERIMENTAL SETUP

Aluminium 1050 alloy sheets of  $300 \text{ mm} \times 200 \text{ mm} \times 3 \text{ mm}$  with smooth surface finishing were used for this research work. These materials were manufactured and supplied by Metal Tool and Trade, South Africa. The chemical composition of the aluminium alloy is 0.05% Manganese, 0.04% Iron, 0.05% Copper, 0.05% Magnesium, 0.25% Silicon, 0.07% Zinc, 0.05% Titanium and 99.49%

Aluminium. Before the welding process, V-grooves with depth of 1.5 mm and width of 3 mm were made on all the aluminium sheets using a milling machine and the titanium carbide particles were filled and compacted into the grooves. A cylindrical H13 steel tool hardened to 52 HRC was used for the welding. A basic tool geometry was used with a tool length of 5.7 mm and tool diameter of 6 mm. The tool shoulder diameter is thrice the pin diameter (18 mm) and concave in geometry to exert pressure on the workpiece during welding. The welding was performed on an Intelligent Stir Welding for Industry and Research (I-STIR) Process Development System (PDS), The FSW platform used is capable of capturing the forces and torque output and the block diagram of the input and output process parameters is illustrated in Figure 2. Tilt angle of  $3^\circ$  was kept constant and used throughout the welding. The rotational and the transverse speeds employed in this research study are presented in Table 1. Also shown in Table 1 is the weld number assigned to each sample and the weld pitch, which is the ratio of transverse speed to the rotational speed and the composition of the weld surface.

TABLE 1  
FSW PROCESS PARAMETERS

Weld number	Rotational Speed (rpm)	Transverse Speed (mm/min)	Weld interface composition	Weld Pitch (mm/rpm)
A1	1600	100	With TiC	0.063
A2	1600	200	With TiC	0.125
A3	1600	300	With TiC	0.188
B1	1800	100	With TiC	0.056
B2	1800	200	With TiC	0.111
B3	1800	300	With TiC	0.167
C1	2000	100	With TiC	0.050
C2	2000	200	With TiC	0.100
C3	2000	300	With TiC	0.150
D1	1600	200	Without TiC	0.125
D2	1800	200	Without TiC	0.111
D3	2000	200	Without TiC	0.100

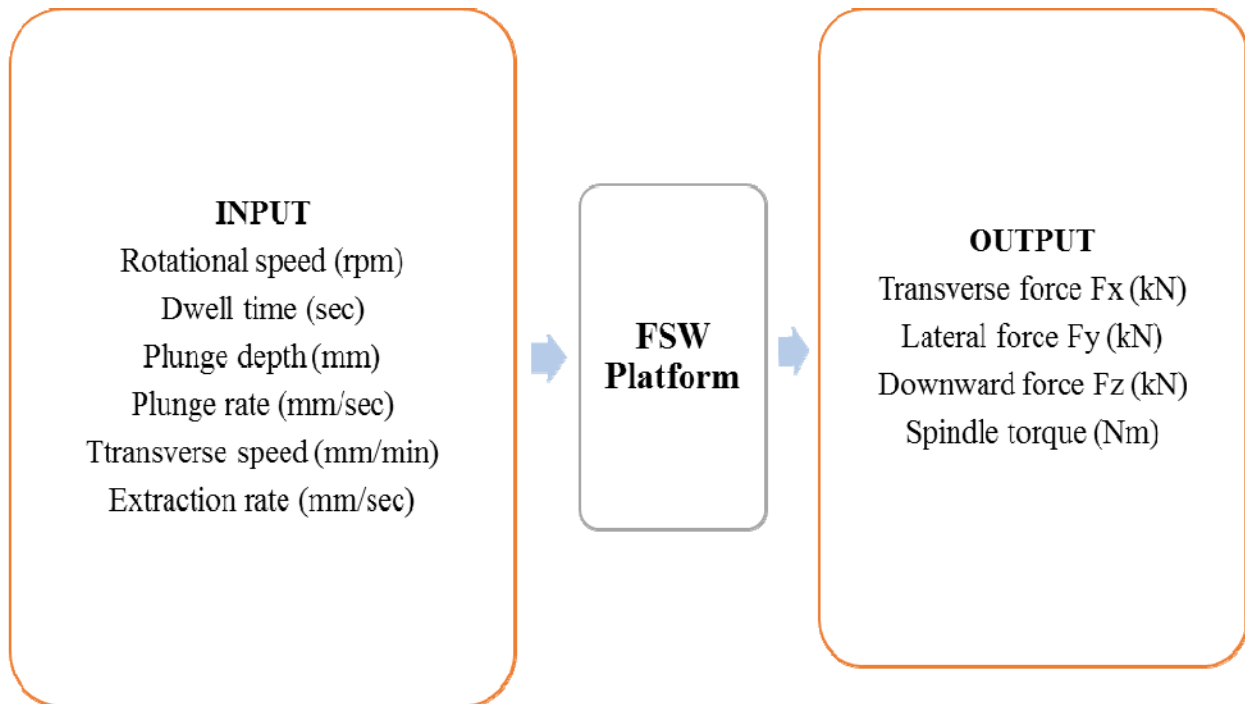


Figure 2 Block diagram of the input and output feedback on FSW platform

### III. RESULT AND DISCUSSION

This section discusses the results obtained on the FSW Platform

#### A. Output Response Feedback

During welding, the output response parameters ( $F_x$ ,  $F_y$ ,  $F_z$  and Torque) that acted on the workpieces were captured and are presented in Table 2.

The data presented in Table 2 were taken in the welding state (steady state) region when all the welding parameters

are nearly constant i.e. the period during which the force, torque and heat output reach a near equilibrium state. Once the thermal equilibrium has been reached, these output response parameters become constant.

A typical force-time graph recorded is shown in Figure 3. The pre-welding state (unsteady state) and welding state (steady state) can be easily identified from the graph. The pre-welding state is associated with surge and variations in the forces feedback.

TABLE 2  
AVERAGE OUTPUT RESPONSE FROM THE FSW PLATFORM

Weld number	Weld Pitch (mm/rpm)	Rotational Speed (rpm)	Transverse Speed (mm/min)	Weld interface orientation	$F_x$ Force (kN)	$F_y$ Force (kN)	$F_z$ Force (kN)	Torque (Nm)	Heat output (J/mm)
A1	0.063	1600	100	With TiC	1.47	-0.29	6.81	14.57	1318.43
A2	0.125	1600	200	With TiC	1.31	-0.20	7.25	15.97	722.56
A3	0.188	1600	300	With TiC	1.18	-0.18	8.43	17.50	527.856
B1	0.056	1800	100	With TiC	1.11	-0.15	6.57	11.90	1211.43
B2	0.111	1800	200	With TiC	1.27	-0.10	7.17	13.96	710.57
B3	0.167	1800	300	With TiC	1.31	-0.24	8.01	15.23	516.81
C1	0.050	2000	100	With TiC	0.89	-0.18	5.75	10.67	1206.91
C2	0.100	2000	200	With TiC	1.05	-0.11	6.78	12.08	683.19
C3	0.150	2000	300	With TiC	1.27	-0.08	7.25	14.58	549.72
D1	0.125	1600	200	Without TiC	2.34	-0.19	6.59	16.31	737.94
D2	0.111	1800	200	Without TiC	1.27	-0.14	5.98	14.99	763.00
D3	0.100	2000	200	Without TiC	1.17	-0.15	5.49	13.65	771.99

This is caused by contact between the tool and the workpieces as the tool plunges into the workpiece in an axial direction. However, the forces in the welding stage show less variation and improved uniformity as the tool traverses along the weld seam. From the graph, the highest level of force feedback is associated with the downward force in the z-direction, followed by the transverse force in the x-direction and the least was observed as the lateral force in the y-direction.

The heat input was calculated using equation 1. This is given by Lambard [14]

$$Q = \eta \frac{2\pi\omega T}{v} \quad (1)$$

Where

Q= heat input (J/mm)

$\eta$ = efficiency factor = 0.9 for Aluminium

$\omega$ = rotational speed (rev/min)

v= Transverse speed (mm/min)

T= Torque (Nm)

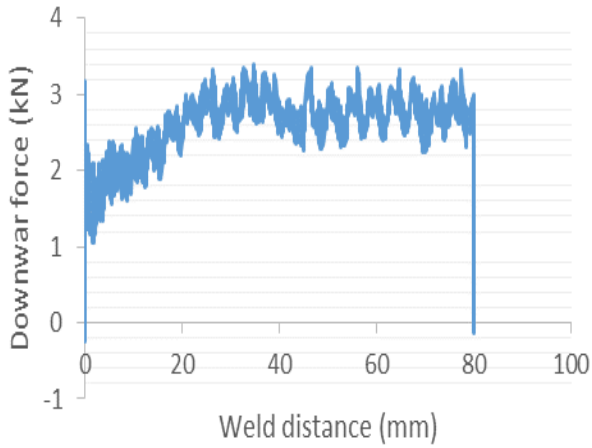


Figure 3 Output downward force  $F_z$  at rotational speed of 2000 rpm and transverse speed of 100 mm/min

As the heat input decreases during welding, the magnitude of the resultant downward force  $F_z$  acting on the workpiece increases.

#### B. Effect of Transverse Speed on Output Response

It should be noted that all the welds produced at the lowest transverse speed of 100 mm/min have the highest heat input as expected since the heat input is dependent on the travel speed. This is due to the fact that at low transverse speed of 100 mm/min, the shoulder of the tool has ample time to interact with the surface of the workpiece, thereby generating more heat compared to the weld produced at 200 mm/min and 300 mm/min respectively. Shown in Figure 4 is the graph of forces feedback against the transverse speed. It was observed that the required forces needed to produce a good weld increase as the transverse speed increases. This is caused by low interaction time at higher transverse speed which led to low heat input and high required forces.

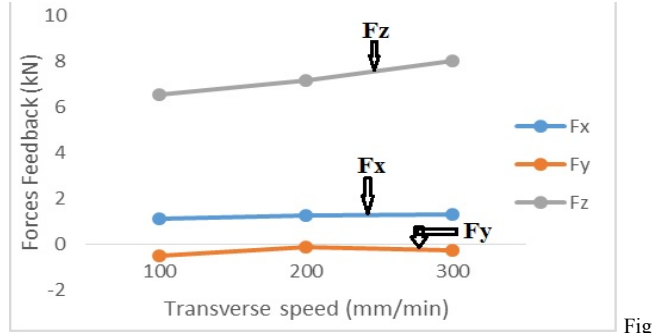


Figure 4 Forces feedback against the transverse speed for samples with reinforcement

#### C. Effect of Rotational Speed on Output Response

From the data obtained, it was observed that as the rotational speed increases, the torque and  $F_z$  force decrease. Since the magnitude of the output  $F_z$  force is determined by the resistance of the material to the motion of the tool, it can be said that increase in the rotational speed led to an increase in the heat input, thereby reducing the amount of force required. Figure 5 shows the graphical representation of  $F_x$ ,  $F_y$  and  $F_z$  against the rotational speed.

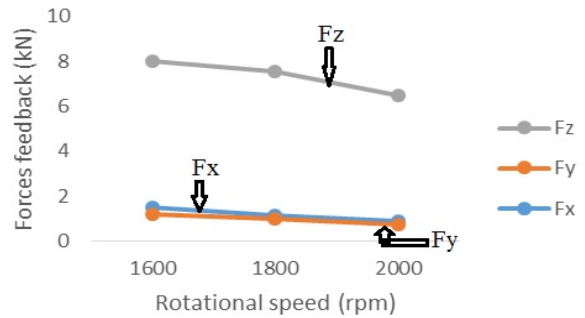


Figure 5 Forces feedback against the rotational speed for samples with reinforcement

Long et al [15] reported that torque decreases with increasing rotation speed due to higher temperature caused by higher heat generation rate (heat input/time), whose indicator is power input, which was observed also.

#### D. Influence of Reinforcement Particles on the Downward Force Output and Torque

Shown in Figure 6 is the comparison of the downward force  $F_z$  and Figure 7 illustrated the torque response generated at weld with and without reinforcement. It was noticed that with the same input process parameter for welds A2 and D1, B2 and D2 and C2 and D3, the output parameters were different. This shows that the composition of the material is also a factor that determines the output response. The output downward force  $F_z$  in welds A2, B2 and C2 are higher due to presence of TiC particles which in turn lowers heat input compared to D1, D2 and D3 since the heat input is a major determinant of  $F_z$ . The opposite of  $F_z$  was observed for the torque outputs. The torque outputs in the welds without reinforcement are higher. This shows that the relationship

between the downward force  $F_z$  and torques is inverse. As the downward force increases, the torque output decreases.

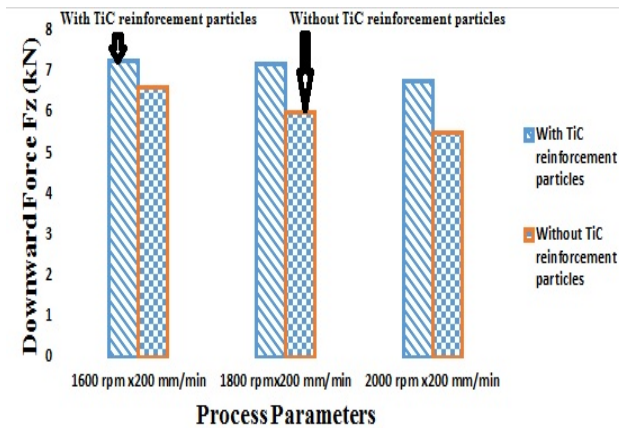


Figure 6 Comparison of downward force feedback for welds with and without reinforcement particle

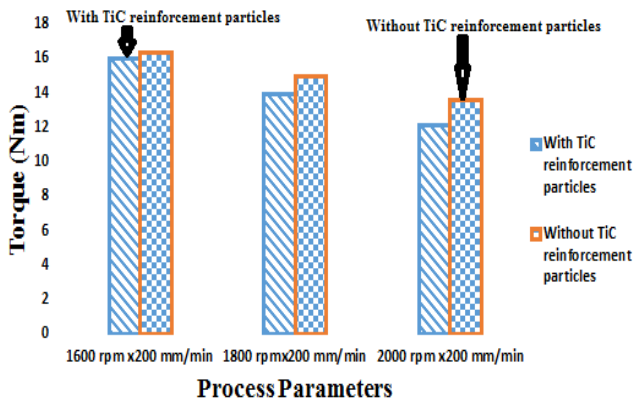


Figure 7 Comparison of torque outputs for welds with and without reinforcement particles

#### IV. CONCLUSION

It can be concluded that the the input parameters (rotational and transverse speeds) and the composition of the workpiece have an effect on the output response. As the rotational speed increases, the forces feedback decreases and vice versa but for the traverse speed, the observation is completely opposite. An increase in the transverse speed caused increase in forces feedback. It was also observed that the composition of the workpiece affects the required force for welding. At weld seam with reinforcement particles, higher force input was required to join the workpieces together.

#### NOMENCLATURES

Q	heat input
$\eta$	Efficiency factor = 0.9 for Aluminium
$\Omega$	rotational speed (rev/min)
$v$	Transverse speed (mm/min)
T	Torque
$F_x$	Transverse force
$F_y$	Lateral force
$F_z$	Downward force

#### ACRONYMS

FSW Friction stir welding

#### ACKNOWLEDGMENT

The authors would like to acknowledge the eNtsa Research Group of Nelson Mandela Metropolitan University (NMMU), Port Elizabeth, South Africa for allowing us to use their facility to produce the welds.

#### REFERENCES

- [1] R. S. Mishra and Z. Ma, "Friction stir welding and processing," *Materials Science and Engineering: R: Reports*, vol. 50, pp. 1-78, 2005.
- [2] K. S. Arora, S. Pandey, M. Schaper and R. Kumar, "Effect of process parameters on friction stir welding of aluminum alloy 2219-T87," *The International Journal of Advanced Manufacturing Technology*, vol. 50, pp. 941-952, 2010.
- [3] M. Besharati-Givi and P. Asadi, *Advances in Friction-Stir Welding and Processing*. Elsevier, 2014.
- [4] C. Rowe and W. Thomas, "Advances in tooling materials for friction stir welding," *TWI and Cedar Metals Ltd*, pp. 1-11, 2005.
- [5] A. Arora, R. Nandan, A. Reynolds and T. DebRoy, "Torque, power requirement and stir zone geometry in friction stir welding through modeling and experiments," *Scr. Mater.*, vol. 60, pp. 13-16, 2009.
- [6] E. T. Akinlabi, *Characterisation of Dissimilar Friction Stir Welds between 5754 Aluminium Alloy and C11000 Copper*, 2011.
- [7] E. T. Akinlabi, "Friction stir welding: Evolution and advances," 2nd international conference on advances in cutting, welding and surfacing, Coimbatore, pp 39-48, India, 2015.
- [8] K. J. Colligan and R. S. Mishra, "A conceptual model for the process variables related to heat generation in friction stir welding of aluminum," *Scr. Mater.*, vol. 58, pp. 327-331, 2008.
- [9] C. Blignault, D. Hattingh, G. Kruger, T. Van Niekerk and M. James, "Friction stir weld process evaluation by multi-axial transducer," *Measurement*, vol. 41, pp. 32-43, 2008.
- [10] W. Arbegast "R. S. Mishra and M. W. Mahoney, *Friction Stir Welding and Processing*". ASM international, 2007.
- [11] C. Blignault, D. Hattingh and M. James, "Optimizing friction stir welding via statistical design of tool geometry and process parameters," *Journal of Materials Engineering and Performance*, vol. 21, pp. 927-935, 2012.
- [12] T. Long and A. P. Reynolds, "Parametric studies of friction stir welding by commercial fluid dynamics

simulation," *Science and Technology of Welding & Joining*, vol. 11, pp. 200-208, 2006.

- [13] N. Balasubramanian, B. Gattu and R. S. Mishra, "Process forces during friction stir welding of aluminium alloys," *Science and Technology of Welding & Joining*, vol. 14, pp. 141-145, 2009.
- [14] H. Lambard, "Optimized fatigue and fracture performance of friction stir welded aluminium plate: A study of the inter-relationship between process parameters, TMAZ, microstructure, defect population and performance. PhD Thesis. University of Plymouth, England." 2007.
- [15] T. Long, W. Tang and A. Reynolds, "Process response parameter relationships in aluminium alloy friction stir welds," *Science and Technology of Welding & Joining*, vol. 12, pp. 311-317, 2007.